actuators

MDPI

Review

Recent Structure Development of Poly(vinylidene fluoride)-Based Piezoelectric Nanogenerator for Self-Powered Sensor

Cheoljae Lee †, Hyosik Park † and Ju-Hyuck Lee *

Department of Energy Science and Engineering, Daegu Gyeongbuk Institute of Science and Technology (DGIST), Daegu 42988, Korea; kum3223@dgist.ac.kr (C.L.); parkhyo63@dgist.ac.kr (H.P.)

* Correspondence: jhlee85@dgist.ac.kr

† These authors contributed equally to this work.

Received: 30 June 2020; Accepted: 20 July 2020; Published: 22 July 2020

Abstract: As the internet of things (IoT) era approaches, various sensors, and wireless electronic devices such as smartphones, smart watches, and earphones are emerging. As the types and functions of electronics are diversified, the energy consumption of electronics increases, which causes battery charging and maintenance issues. The piezoelectric nanogenerator (PENG) received great attention as an alternative to solving the energy issues of future small electronics. In particular, polyvinylidene fluoride (PVDF) piezoelectric polymer-based PENGs are strong potential candidate with robust mechanical properties and a high piezoelectric coefficient. In this review, we summarize the recent significant advances of the development of PVDF-based PENGs for self-powered energy-harvesting systems. We discuss the piezoelectric properties of the various structures of PVDF-based PENGs such as thin film, microstructure, nanostructure, and nanocomposite.

Keywords: energy harvesting; piezoelectric; nanogenerator; polyvinylidene fluoride

1. Introduction

Due to the recent miniaturization of electronic devices and the addition of various functions, it is insufficient to supply power only with a battery. Therefore, energy harvesting technology that converts environmental energy into electrical energy is attracting attention, in particular, piezoelectric nano generators (PENGs), that convert mechanical energy into electrical energy, are in the spotlight. The piezoelectric effect, discovered by Jacques Curie and Pierre Curie in 1880, is the phenomenon of electricity generation when external pressure is applied to a piezoelectric material [1,2] that has a non-centrosymmetric crystal structure [3]. It is known that the piezoelectric effect appears when the polarization strength changes as the dipole moment changes due to external stress [4]. If electrodes are placed on both sides of the piezoelectric material, electrons flow through the external circuit to reduce the potential difference caused by the changed polarization. When the applied pressure is released, the polarization returns to its original state, and the electrons return to their original state through the external circuit. This process produces piezoelectric voltage and current from the PENG. Over the decades, various materials for high performance piezoelectric elements have been studied. Inorganic piezoelectric materials such as zinc oxide (ZnO) [5–10], lead zirconate titanate (PZT) [11–14], lead magnesium niobate-lead titanate (PMN–PT) [15–17], and barium titanate ($BaTiO_3$) [18–20], as well as organic materials such as polyvinylidene fluoride (PVDF), poly(vinylidenefluoride–co–trifluoroethylene) (P(VDF–TrFE)) [21–23], nylon [24], diisopropylammonium bromide [25], and biomolecular materials [26–28] have been developed. Compared to inorganic piezoelectric materials, organic piezoelectric material has various

advantages such as high flexibility, light weight, long-term stability, and an easy fabrication process. Among the various organic piezoelectric materials, PVDF has received much attention because of its high piezoelectric coefficient, transparency, mechanical durability, and flexibility. It was demonstrated that the PVDF-based PENGs offer multifunctionalities such as high sensitivity, flexibility, stretchability, and multi-shape transformability for the stable and continuous operation of self-powered sensors [29–32]. In recent years, numerous studies on the various types of PENGs based on diverse PVDF structures have been reported (Figure 1). In this review, we introduce the recent advances of various structure fabrications of piezoelectric PVDF, and structure-dependent piezoelectricity. In addition, we discuss the piezoelectric output performance of PENGs based on various structures of PVDF-based nanogenerators such as thin film, microstructure, nanostructure, and nanocomposites.

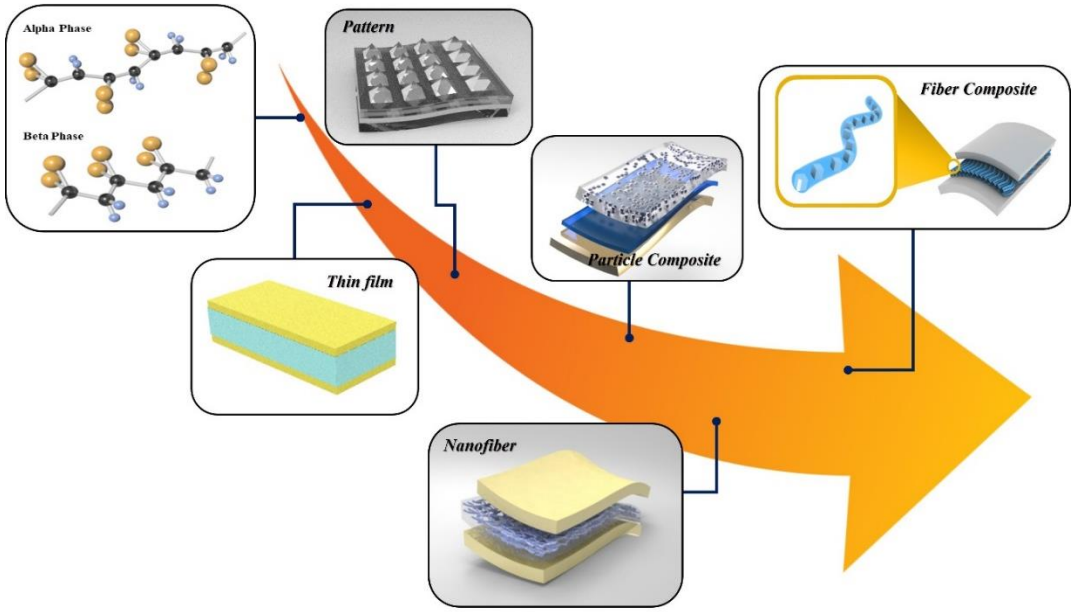

Figure 1. A schematic illustration of the various structured polyvinylidene fluoride (PVDF)-based piezoelectric nanogenerators.

2. Thin Film PVDF Structure

The most simple and traditional PENG structure is composed of bulk or a thin film base. Thin-film PVDF has advantages in flexibility and electrical output compared to bulk PVDF. Accordingly, various thin-film PVDF-based PENGs have been reported [33–43].

In 2014, Pi et al. reported an poly(vinylidenefluoride–co–trifluoroethylene) (P(VDF–TrFE)) thin-film-based PENG for a flexible nanogenerator [44]. A gold (Au) layer was deposited as a lower electrode on a silicon dioxide layer deposited on polyimide (PI) substrate. The P(VDF–TrFE) solution was spin coated on a lower electrode, and Au was deposited on a P(VDF–TrFE) thin film again as an upper electrode (Figure 2a). The manufactured P(VDF–TrFE)-based PENG was electrically poled by the application of an external electric field with a strength of 0.5–0.8 MV/cm. The output performance of the PENG was increased as the alignment of the polarization direction by the poling process due to exhibiting ferroelectric property as shown in the polarization–electric field (P–E) curve (Figure 2b). The output performance of the P(VDF–TrFE) thin-film-based PENG was measured with the repetition of a stretching and releasing process. The PENG produced an output voltage and current of 7 V and 58 nA, respectively, when a strain of 0.943% was applied with a frequency of 0.5 Hz. As the applied frequency and strain increased, the output voltage and current of the PENG also increased (Figure 2c).

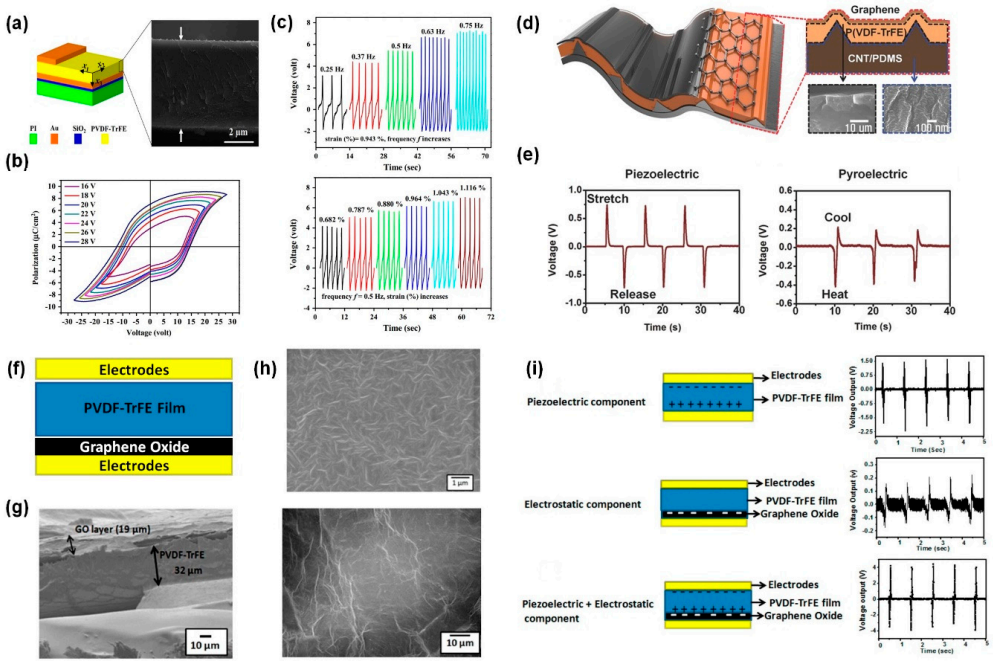

Figure 2. (**a**) A schematic of the thin film piezoelectric nano generator (PENG) and cross-sectional SEM image of a PVDF thin film. (**b**) Polarization versus the applied voltage hysteresis loop of the PVDF thin film. (**c**) The open-circuit voltage with a different frequency at a fixed strain magnitude of 0.943% (up) and a different magnitude at the fixed frequency of 0.5 Hz (down). [44] Copyright 2014, Elsevier Ltd. (**d**) Schematic illustration of a stretchable hybrid nanogenerator and SEM images of the poly(vinylidenefluoride–co–trifluoroethylene) (P(VDF–TrFE)) thin film. (**e**) Piezoelectric output voltage during the stretching–releasing cycle and pyroelectric output voltage during the heating–cooling cycle. [45] Copyright 2013, John Wiley and Sons. (**f**) A schematic illustration of the P(VDF–TrFE)/graphene oxide (GO) bilayer nanogenerator. (**g**) Cross-sectional SEM image of the P(VDF–TrFE)/GO bilayer film. (**h**) Surface morphology SEM image of the P(VDF–TrFE)/GO bilayer film. (**i**) Working mechanism and output voltage of the thin film PENGs. [46] Copyright 2016, American Chemical Society.

In 2013, Lee et al. reported a highly stretchable nanogenerator (HSNG) for mechanical and thermal energy harvesting based on P(VDF–TrFE) thin film [45]. The HSNG consists of three layers: a patterned polydimethylsiloxane-carbon nanotube (PDMS–CNT) which acts as the bottom electrode, P(VDF–TrFE) as the piezoelectric and pyroelectric polymer and graphene as the top electrodes (Figure 2d). Since the HSNG is very elastic, flexible, and stretchable, it can be used as a power source for various flexible and stretchable electronics. In addition, the efficiency of pyroelectric power generation is increased by using a high thermal conductive graphene electrode. The measured piezoelectric output voltage was 0.7 V by 30% of the stretching–releasing cycle, and the measured pyroelectric output voltage was 0.4 V by the heating–cooling (ΔT = 30 °C) cycle (Figure 2e). The measured output voltage was 1.1 V when the piezoelectric and pyroelectric effects were hybridized by a coupling phenomenon. In addition, the HSNG was mechanically stable up to the strain of 30%.

In 2016, Bhavanasi et al. reported a bilayer piezoelectric nanogenerator that added a graphene oxide (GO) layer to a P(VDF–TrFE) film to enhance Young's modulus and the piezoelectric properties (Figure 2f) [46]. The PENG was fabricated by the drop casting of the P(VDF–TrFE) and GO solution on the indium tin oxide (ITO) electrode, and Au was deposited on the P(VDF–TrFE) layer as an upper electrode. The thickness of the GO and P(VDF–TrFE) layer was about 19 μm and 32 μm, respectively. The fabricated PENG is flexible enough for bending or rolling. The P(VDF–TrFE)–GO bilayer PENG produced the maximum output voltage and current of 4.26 V and 1.88 μA, respectively, whereas the P(VDF–TrFE) monolayer-based PENG only produced an output voltage and current of 2.1 V and 0.96 μA under the compression pressure of 0.32 MPa (Figure 2g), respectively. In the case of the

P(VDF–TrFE) monolayer, the mechanical–electrical conversion efficiency of the PENG was determined by the direct influence of the P(VDF–TrFE) intrinsic permittivity and Young's modulus. However, in the case of the P(VDF–TrFE)–GO double layer, not only the effect of GO's dielectric constant and Young's modulus but also the electrostatic effect were combined to increase the mechanical–electrical conversion efficiency by two times the output voltage and 2.5 times the output power.

3. Micro Scale PVDF Structure

The microstructure of the PVDF improves the output performance of PENG because of the stress concentration effect even with small force. Therefore, microporous [47–52], micropatterns [53–60], micropillars [61–65], and microfiber [66–70] structured PVDF have been developed to improve the output performance of PENGs.

In 2014, Chen et al. reported a microporous PVDF-based PENG [71]. Figure 3a shows a schematic illustration of the microporous PVDF-based PENG, which was composed of kapton substrate, bottom electrode, porous PVDF and upper electrode. The microporous film was fabricated by the solvent evaporation method. The porous surface increases the compressibility of PVDF, and the piezoelectric constant is proportional to the compressibility, Equations (1) and (2), and results in the increased output performance of the PENG:

$$d_{ij} = \frac{\partial}{\partial T_j} = \frac{\partial \mu_i}{\partial T_j}\left(\frac{1}{V}\right) - \frac{\mu_i}{V^2}\left(\frac{\partial V}{\partial T_j}\right) \quad (1)$$

$$c_j = -\frac{1}{V}\frac{\partial V}{\partial T_j} \quad (2)$$

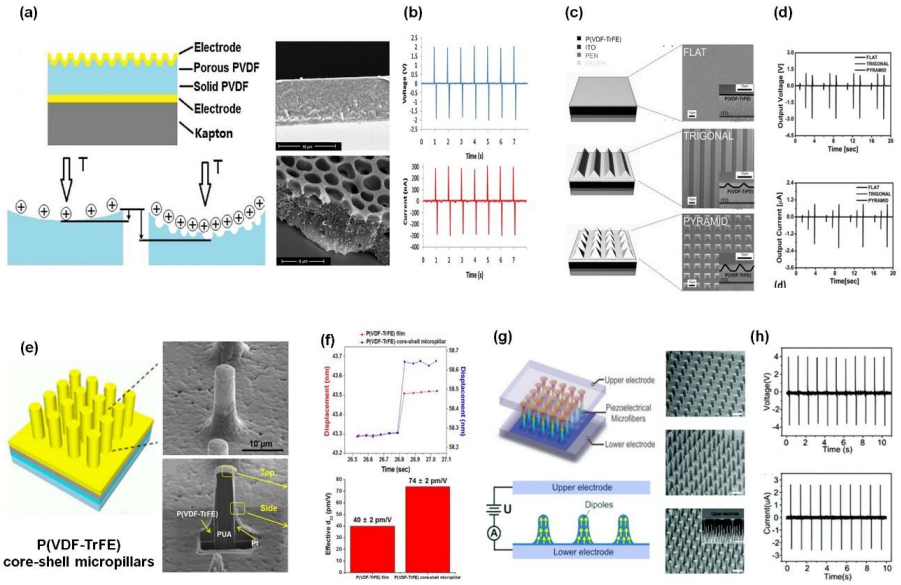

Figure 3. (**a**) Schematic illustration and SEM images of the mesoporous surface PVDF-based PENG. (**b**) Output voltage and current of the mesoporous PVDF PENG. [71] Copyright 2014, Elsevier. (**c**) Schematic diagrams and SEM images of the flat, trigonal-line shape, and pyramid-shaped P(VDF–TrFE)-based PENGs. (**d**) Experimentally observed output voltage and the current of the flat, trigonal-line shape, and pyramid-shaped P(VDF–TrFE)-based PENGs. [72] Copyright 2015, WILEY-VCH. (**e**) A schematic image and the SEM images of P(VDF–TrFE) core-shell micropillars. (**f**) The displacement changes and piezoelectric constants d_{33} of the P(VDF–TrFE) film and P(VDF–TrFE) core-shell micropillar. [73] Copyright 2015, Springer Nature. (**g**) Schematic images of the PVDF microfiber-based PENG and SEM images of the PVDF microfiber. (**h**) Measured output voltage and the current signals of the microfiber-based PENG. [74] Copyright 2015, The Royal Society of Chemistry.

The output performance of the microporous PVDF film-based PENGs was measured by compression and tension at 1 Hz by bending. Bare PVDF film (0:5 = acetone:methyl ethyl ketone) produced an output voltage of 0.8 V and an output current of 160 nA. The microporous PVDF film-based PENGs (3:2 = acetone:methyl ethyl ketone) produced an output voltage of 2 V and an output current of 300 nA under the same conditions due to the increased compressibility (Figure 3b). In addition, the porous PENG produced sufficient energy to charge a 1 μF capacitor up to 1.7 V for 360 cycles that showed two times the improved performance compared to the bare PVDF film PENG (0.82 V).

In 2015, Lee et al. reported a micropattern P(VDF–TrFE)-based PENG for a mechanical stimuli sensor system [72]. Micropatterned P(VDF–TrFE) is fabricated using the Si mold made by simple photolithography and chemical etching process. The trigonal line-shaped and pyramid-shaped micropatterned PVDF was fabricated on the ITO-coated polyethylene naphthalate (PEN) substrate, and the Ag electrode was deposited on top of the patterned P(VDF–TrFE) (Figure 3c). Due to the patterned structure, the piezoelectric element can be highly deformed by vertical pressure, thereby improving the piezoelectric output performance. The output performance of the micropattern PENGs was measured by applying a vertical compressive force at the top of the PENG using a mechanical force stimulator. The piezoelectric output voltages and currents of a flat, trigonal line, and pyramid-patterned PENG were 0.4, 2.0, and 2.9 V, and 100, 500, and 900 nA, respectively, under the vertical compressive force of 1.5 N, as shown in Figure 3d. In addition, the output voltage and current were 4.4 V and 3.4 μA for the pyramid-shaped PENG at 16 N. The pyramidal patterned P(VDF–TrFE)-based PENGs exhibited a five times stronger output than the flat P(VDF–TrFE)-based PENGs. In practical application, the pyramidal pattern-based PENG can detect extremely low wind speeds of 0.5 m/s and can be used as self-powered active pressure sensors.

In 2015, Choi et al. reported vertically aligned P(VDF–TrFE) core-shell structures for PENG [73]. The P(VDF–TrFE) layers were coated onto the platinum/polyurethane acrylate (PUA) pillars and the Pt layer was subsequently deposited on the P(VDF–TrFE) layer (Figure 3e). This micro-sized pillar structure is also easier to deform than film by external mechanical force, thus improving the piezoelectric efficiency. In order to evaluate the piezoelectric properties of the core-shell structure P(VDF–TrFE), the reverse piezoelectric effect was measured by using voltage-displacement analysis. The displacement of the nanoindentation tip in contact with a 1 μm-thick micropillar was measured with a position accuracy of 0.01 nm. A voltage via of 5 V was applied between the tip and bottom electrodes. The P(VDF–TrFE) film showed a displacement of 0.2 nm, and the P(VDF–TrFE) core-shell micropillar showed a displacement of 0.37 nm. The average values of d_{33} of the P(VDF–TrFE) film and the P(VDF–TrFE) core-shell micropillar were (40 ± 2) pm/V and (74 ± 2) pm/V, respectively (Figure 3f). The core-shell micropillar structure showed a 1.85-fold improvement in piezoelectric constant d_{33} compared to the flat film.

In 2015, Chen et al. reported a microfiber PENG with vertically aligned P(VDF–TrFE) [74]. The P(VDF–TrFE) microfiber PENG was used to harvest the mechanical energy and operate the luminescent electronic devices. The vertically aligned P(VDF–TrFE) microfiber with 8 μm in diameter and 50 μm in height were fabricated by the electrohydrodynamically (EHD) pulling method. The P(VDF–TrFE) microfibers are vertically connected to both top and bottom electrodes (Figure 3g). The piezoelectric output performances of 10 mm x 10 mm of the PENG were measured using an electrochemical vibrator with a 25 N force and 1 Hz of frequency. The peak output voltage and current were 4 V and 2.6 μA, respectively (Figure 3h). The P(VDF–TrFE) microfiber PENG was able to charge the 47 μF capacitor to 5.1 V for 270 s and drive a four-bit liquid crystal display (LCD). In addition, it was able to control its output performance by controlling the diameter and shape of the P(VDF–TrFE). Since the air gap between the fibers makes the array structure porous, hence increasing the stress on the piezoelectric material. The finite element method (FEM) simulation performed to evaluate the effect of the diameter and shape of the P(VDF–TrFE) on the piezoelectric effect.

4. Nano Scale PVDF Structure

The nanostructured PVDF also exhibit structure-dependent piezoelectricity. Consequently, various types of PVDF nanostructures, such as nanoporous [75–79], nanofiber [80–86], and nanotube [87–90] have been reported.

In 2014, Mao et al. reported a mesoporous PVDF for a scalable PENG and self-powered electronic system [91]. Mesoporous PVDF thin film was prepared by casting a mixture of ZnO nanoparticle and PVDF solution, and then removing the ZnO nanoparticle with HCl solution (Figure 4a). The HCl solution was chosen because the PVDF is a hydrophobic polymer with good chemical stability against corrosive solvent-containing acids. The ZnO nanoparticles create porosity in the PVDF films and help the PVDF to form a piezoelectric β-phase. The open-circuit voltage and short-circuit current were measured under a 40 Hz condition. The mesoporous PVDF-based PENG produced an 11.0 V average output voltage and 9.8 μA output current (Figure 4b). This output performance is much higher than that of the bare PVDF bulk film (5.0 V). The conversion efficiency of the mesoporous PVDF PENG improved as the ZnO mass fraction increased up to 50%, but decreased at a higher ratio due to the formation of the decreased β-phase (Figure 4c). The optimal porosity for achieving the maximum V_{oc} output was identified to be –11.0 V. As a demonstration, parallelly connected four PVDF PENGs are attached on the back of the phone. When the oscillator was turned on, the PENG underneath was activated by the phone's weight, and the generated electricity can charge a 47 μF capacitor to 3.7 V.

In 2010, Chang et al. reported a PVDF nanofiber-based PENG for mechanical energy harvesting [80]. PVDF single nanofiber was prepared using the near field electrospinning method (Figure 4c). The crystal structure of the nanofiber was transformed into polar β-phase by strong electric fields (greater than 10^7 V/m) and stretching forces during the electrospinning process. The electrospun PVDF nanofibers have a diameter from 500 nm to 6.5 μm. The measured piezoelectric output voltage and current from the PVDF single nanofiber-based PENG were 5−30 mV and 0.5−3 nA, respectively, under an applied 0.085% of strain at 2 Hz (Figure 4d). The energy conversion efficiency of the PENG was calculated as the ratio between the generated electrical energy and the applied mechanical energy. The energy conversion efficiency of the nanofiber PENG was found to be as high as 21.8% with an average of 12.5%, which was much greater than conventional PVDF thin films PENG (0.5–2.6%) under the same conditions (Figure 4e) due to the higher crystallinity and sensitivity [84].

In 2014, Bhavanasi et al. reported P(VDF–TrFE) nanotube-based PENGs synthesized by nanoconfinement effect for mechanical energy harvesting [92]. PVDF nanotubes are prepared using an anodic aluminum oxide (AAO) template with a pore diameter of 200 nm. Due to the surface energy of the AAO wall, which is higher than that of the P(VDF–TrFE), the P(VDF–TrFE) is perfectly wetting on the AAO surface to form a uniformly shaped P(VDF–TrFE) nanotube. The fabricated P(VDF–TrFE) nanotube enhanced the ferroelectric phase (β-phase) formation and the reduced structural defects in the nanostructures formed from nanoconfinement in template pores, resulting in higher piezoelectric coefficients compared to bare films. The P(VDF–TrFE) nanotube PENG was prepared by depositing Au on both sides of the P(VDF–TrFE) as the upper and lower electrodes, following the encapsulation with poly(methyl methacrylate) (PMMA) to prevent gold penetration and device electric shortage (Figure 4g). The ferroelectric properties of the P(VDF–TrFE) nanotubes embedded in AAO were confirmed through the polarization–electric field (P–E) curve that shows strong ferroelectric behavior (Figure 4h). The output performance of the P(VDF–TrFE) nanotube and thin-film PENGs were measured under a force of 0.075 MPa and a frequency of 1 Hz. The maximum performance of the P(VDF–TrFE)-nanotube PENG was 4.8 V of open circuit voltage and 2.2 μW/cm^2 of power density. On the other hand, the output performance of the P(VDF–TrFE)-film PENG was only 0.3 V of voltage and 0.06 μW/cm^2 of power density (Figure 4i).

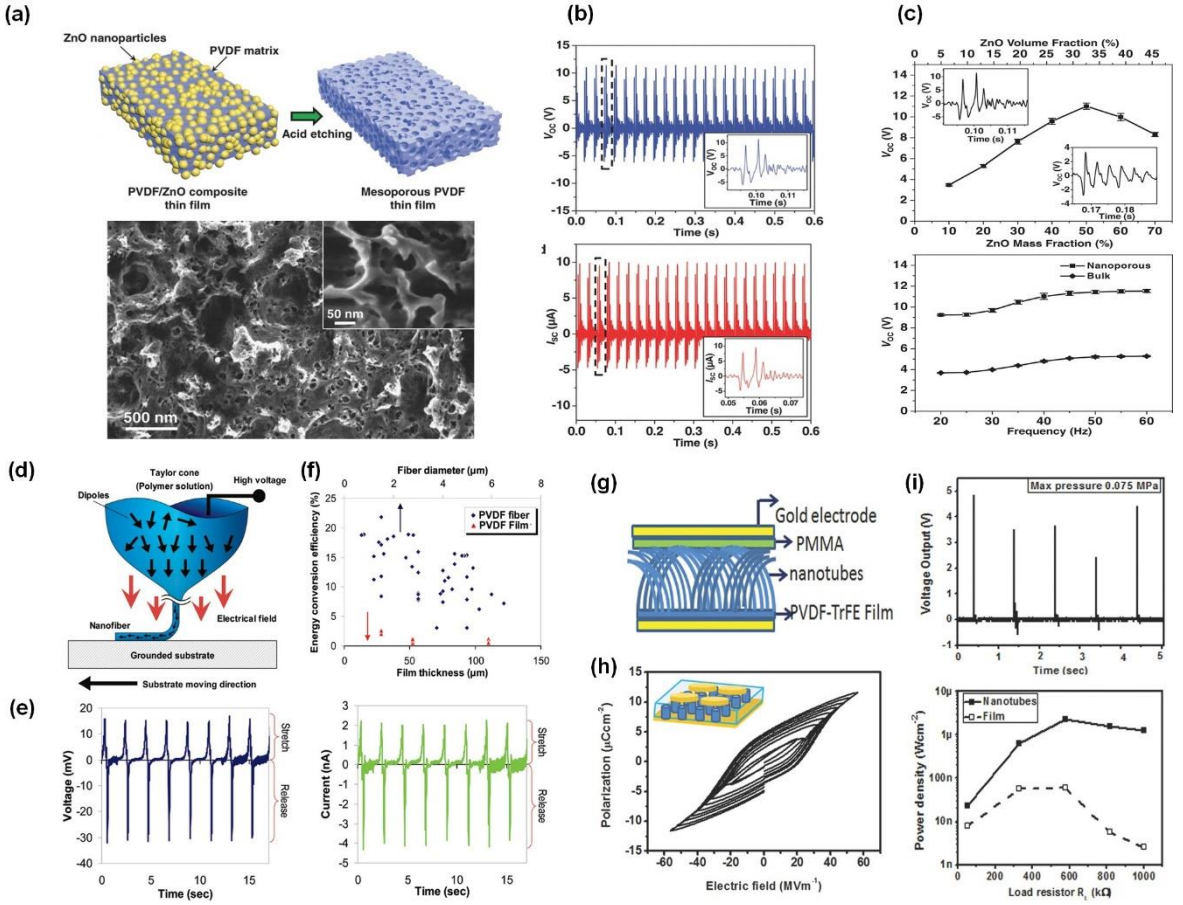

Figure 4. (**a**) Processing and structure of the mesoporous piezoelectric PVDF film, and the SEM image of the mesoporous PVDF film. (**b**) The voltage and current output of the mesoporous PVDF PENG under continuous surface oscillation. (**c**) Porosity-related voltage output. [91] Copyright 2014, WILEY-VCH; (**d**) Schematic image of the PVDF nanofibers fabricated by a near field electrospinning method. (**e**) Measured output voltage and current of the PVDF single nanofiber-based PENG under applied strain at 2Hz. (**f**) Plots of the measured energy conversion efficiency of the PVDF fiber and thin film PENG with different feature sizes. [80] Copyright 2010, American Chemical Society. (**g**) A schematic image of P(VDF–TrFE) nanotube PENG. (**h**) Macroscopic polarization–electric field (P–E) curve hysteresis behavior measured on the P(VDF–TrFE) nanotubes embedded in the anodic aluminum oxide (AAO) template. (**i**) Output voltage of the P(VDF–TrFE) nanotubes PENG, and the output power density under the cyclic load of 0.075 MPa at 1 Hz. [92] Copyright 2014, WILEY-VCH.

5. PVDF Nanocomposite

The PVDF nanocomposite structure with superior piezoelectric inorganic materials such as $BaTiO_3$, PZT, has been developed to enhance the output performance of the PVDF PENGs. In addition, the structure-dependent piezoelectricity of the PVDF nanocomposite such as in the film structure [93–104], micropillar structure [105–109], and nanofiber structure [110–117] were reported.

Alluri et al. reported flexible $BaTi_{(1-x)}Zr_xO_3$(BTZO)/PVDF nanocomposite film PENGs for a self-powered fluid velocity sensor [118]. They synthesized strong piezoelectric ceramic BTZO by the molten salt method and mixed it with PVDF to produce nanocomposite film. Then, the PENG was fabricated by coating Al electrodes on the top and bottom of the nanocomposite film (Figure 5a). The maximum open-circuit voltage and short-circuit current for the BTZO nanocube/PVDF-based PENG were 11.9 V and 1.36 μA, respectively, which are greater than the $BaTiO_3$ (BTO) nanocube/PVDF output of 7.99 V and 1.01 μA (Figure 5b). The improvement of the piezoelectric output performance of the PENG is due to the improved piezoelectric coefficient by mixing with BTZO nanoparticles. The output

performance of BTZO/PVDF-film PENGs was measured with 11 N of mechanical load, applied at 3 Hz, 11 Hz and 21 Hz. As the frequency increased from 3 Hz to 21 Hz, the output voltages and current increased from 5 V and 0.71 µA to 12 V and 1.2 µA, respectively (Figure 5c). The fabricated PENG was used as an active sensor to the detect water velocities in the outlet pipe. The produced average maximum power was 0.2 nW at 31.43 m/s water velocity and increased up to 15.8 nW at 125.7 m/s (Figure 5d).

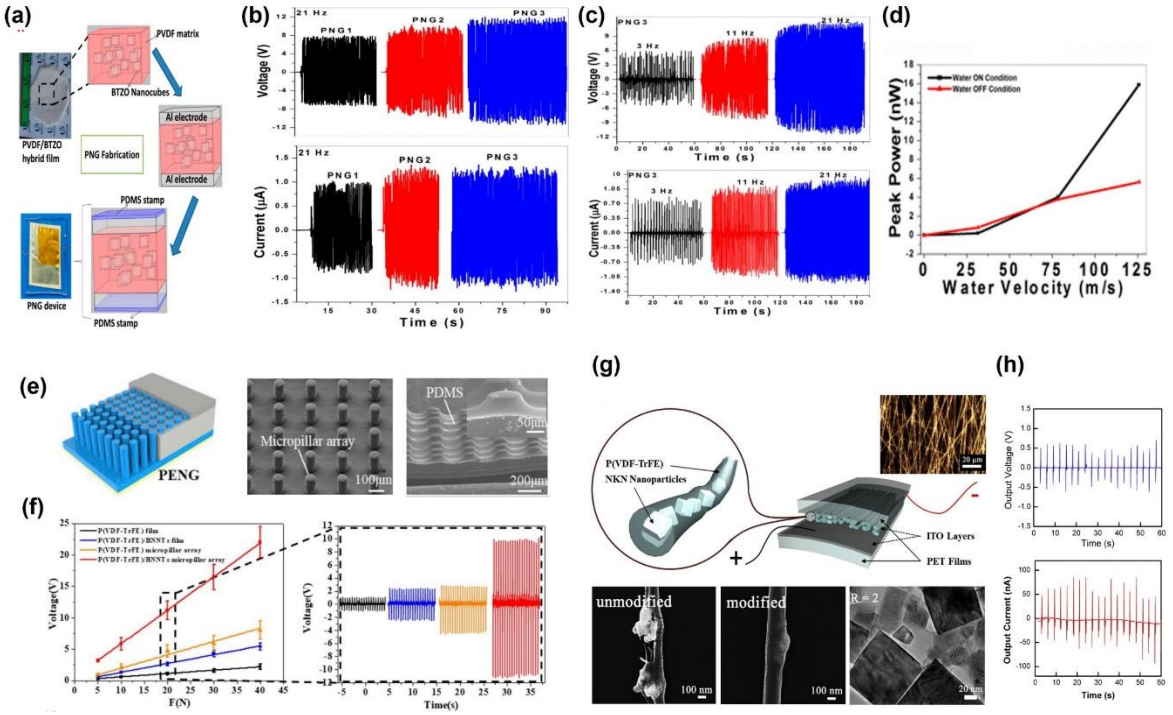

Figure 5. (**a**) Schematic diagram of the key steps of the BZTO/PVDF PENG manufacturing. (**b**) Comparison of the electrical output voltage and the current of the BTO/PVDF, $BT_{(1-x)}Z_{(x)}O$(x = 0.05)/PVDF and $BT_{(1-x)}Z_{(x)}O$(x = 0.1)/PVDF-based PENGs. (**c**) Output voltage and current of the $BT_{(1-x)}Z_{(x)}O$(x = 0.1)/PVDF-based PENG under an external mechanical load (11N) with respect to the cyclic frequency (3, 11, and 21 Hz). (**d**) The generated output peak power obtained at different velocities under the water flow condition. [118] Copyright 2015, American Chemical Society. (**e**) A schematic image of the P(VDF–TrFE)/ boron nitride nanotube (BNNT) nanocomposite micropillar PENG and SEM images of P(VDF–TrFE) nanocomposite micropillars. (**f**) Comparison of the output voltages of the P(VDF–TrFE) thin film, P(VDF–TrFE)/BNNT thin film, P(VDF–TrFE) micropillar, and the P(VDF–TrFE)/BNNT micropillar PENG under different applied force and 20 N force. [119] Copyright 2019, Elsevier Ltd. (**g**) Schematic illustration and SEM images of the $(Na_{0.5}\ K_{0.5})NbO_3$ (NKN)/P(VDF–TrFE) nanofiber-based PENG. (**h**) Output voltage and current of the PENG based on P(VDF–TrFE) nanofiber containing 10 vol% NKN nanoparticles. [120] Copyright © 2015 Elsevier Ltd.

In 2019 Ye et al. reported PENGs based on P(VDF–TrFE)/boron nitride nanotube (BNNT) nanocomposite micropillar for energy harvesting in space [119]. The P(VDF–TrFE)/BNNTs nanocomposite micropillar fabricated using the hot pressed method through the PDMS mold. Then, the PDMS is filled between the micropillars to act as a protective layer (Figure 5e). The improved output performance from the P(VDF–TrFE)/BNNT nanocomposite PENG was observed because BNNT has a higher piezoelectric coefficient and elastic modulus than P(VDF–TrFE). The piezoelectric output performance of the P (VDF-TrFE)/BNNT composite PENG was measured at 2 Hz with an effective area of $1cm^2$ under the compressive force of 40 N. The maximum output voltage and current were 40 V_{pp} and 640 nA, respectively. The output voltage of the bare P(VDF–TrFE) film, P(VDF–TrFE)/BNNT film, P(VDF–TrFE) micropillar, and the P(VDF–TrFE)/BNNT micropillar PENGs were 1 V, 2.6 V, 4.2 V, and

11 V, respectively (Figure 5f). As for the introduced nanocomposite with microarrays structure, the output performance improved 11 times compared to the bare P(VDF–TrFE)-film PENG. The PENG can operate the RYG LED array after charging three capacitors. Moreover, due to the presence of isotope ^{10}B with a high neutron absorption rate, the ability of the BNNTs to shield neutron radiation was experimentally confirmed, showing the possibility of being used as a PENG in space.

Kang et al. reported lead-free piezoelectric ceramic $(Na_{0.5}\ K_{0.5})NbO_3$ (NKN) nanoparticles and P(VDF–TrFE) nanocomposite nanofiber-based PENGs [120]. The nanocomposite nanofiber was prepared by the electrospinning method after the mixing of P(VDF–TrFE) and NKN nanoparticles. The PENG was fabricated by the alignment of the P(VDF–TrFE)/NKN nanocomposite nanofibers in a direction parallel to the upper and lower ITO electrodes (Figure 5g). Due to the strong piezoelectric coefficient of a NKN nanoparticle, the output performance of the nanocomposite PENG was enhanced compared to the bare P(VDF–TrFE) nanofiber-based PENG. The output performance comparison was conducted for PENGs with different NKN concentrations (0 vol%, 5 vol% and 10 vol%). When the device bent, the measured output voltage and current from 0, 5, and 10 vol% nanocomposite PENGs were 0.45 V, 0.64 V, and 0.98 V, and 56 nA, 63 nA and 78 nA, respectively (Figure 5h).

6. Conclusions

The development of various future wireless electronics and sensors requires the development of the high-performance portable power generator. Recently, various studies are under way showing the possibility of supplying sufficient power from the PENGs. The developments of piezoelectric materials with high piezoelectric coefficients and robust physical properties, and an efficient PENG device structure for various applications have been conducted. In this review, recent studies on PENGs with various structures of PVDF and its applications are discussed. To improve the output performance of the PVDF PENGs, the design of the structure of the piezoelectric materials and devices are very critical for the various applications. The materials and devices preparation method and study of the output performance are summarized. To date, many PENG technologies including piezoelectric materials, material structure, and device structure were reported, contributing to the significant increase in the output power. However, further enhancement in the output power was still essential to the commercialization of the PENG. We believe this review can be useful and helpful in the design and development of PENGs that can provide sufficient energy for self-powered electronics.

Author Contributions: Conceptualization, C.L., H.P. and J.-H.L.; formal analysis, C.L.; investigation, H.P.; writing—original draft preparation, C.L. and H.P.; writing—review and editing, J.-H.L.; supervision, J.-H.L. All authors have read and agreed to the published version of the manuscript.

Funding: This work was supported by the National Research Foundation of Korea (NRF) grant funded by the Korea government (MSIT) (No. 2020R1C1C1007436).

Conflicts of Interest: The authors declare no conflict of interest.

References

1. Anton, S.R.; Sodano, H.A. A review of power harvesting using piezoelectric materials (2003–2006). *Smart Mater. Struct.* **2007**, *16*, R1. [CrossRef]
2. Maeder, M.D.; Damjanovic, D.; Setter, N. Lead free piezoelectric materials. *J. Electroceram.* **2004**, *13*, 385–392. [CrossRef]
3. Brown, C.; Kell, R.; Taylor, R.; Thomas, L. Piezoelectric materials, a review of progress. *IRE Trans. Compon. Parts* **1962**, *9*, 193–211. [CrossRef]
4. Sodano, H.A.; Inman, D.J.; Park, G. A review of power harvesting from vibration using piezoelectric materials. *Shock Vib. Dig.* **2004**, *36*, 197–206. [CrossRef]
5. Kim, D.; Lee, K.Y.; Gupta, M.K.; Majumder, S.; Kim, S.-W. Self-compensated insulating ZnO-based piezoelectric nanogenerators. *Adv. Funct. Mater.* **2014**, *24*, 6949–6955. [CrossRef]
6. Xi, Y.; Song, J.; Xu, S.; Yang, R.; Gao, Z.; Hu, C.; Wang, Z.L. Growth of ZnO nanotube arrays and nanotube based piezoelectric nanogenerators. *J. Mater. Chem.* **2009**, *19*, 9260–9264. [CrossRef]

7. Wang, X.; Song, J.; Liu, J.; Wang, Z.L. Direct-current nanogenerator driven by ultrasonic waves. *Science* **2007**, *316*, 102–105. [CrossRef]
8. Lee, Y.; Kim, S.; Kim, D.; Lee, C.; Park, H.; Lee, J.-H. Direct-current flexible piezoelectric nanogenerators based on two-dimensional ZnO nanosheet. *Appl. Surf. Sci.* **2020**, *509*, 145328. [CrossRef]
9. Lee, K.Y.; Bae, J.; Kim, S.; Lee, J.-H.; Yoon, G.C.; Gupta, M.K.; Kim, S.; Kim, H.; Park, J.; Kim, S.-W. Depletion width engineering via surface modification for high performance semiconducting piezoelectric nanogenerators. *Nano Energy* **2014**, *8*, 165–173. [CrossRef]
10. Gupta, M.K.; Lee, J.-H.; Lee, K.Y.; Kim, S.-W. Two-dimensional vanadium-doped ZnO nanosheet-based flexible direct current nanogenerator. *ACS Nano* **2013**, *7*, 8932–8939. [CrossRef]
11. Chen, X.; Xu, S.; Yao, N.; Shi, Y. 1.6 V nanogenerator for mechanical energy harvesting using PZT nanofibers. *Nano Lett.* **2010**, *10*, 2133–2137. [CrossRef]
12. Qi, Y.; Kim, J.; Nguyen, T.D.; Lisko, B.; Purohit, P.K.; McAlpine, M.C. Enhanced piezoelectricity and stretchability in energy harvesting devices fabricated from buckled PZT ribbons. *Nano Lett.* **2011**, *11*, 1331–1336. [CrossRef]
13. Park, K.I.; Son, J.H.; Hwang, G.T.; Jeong, C.K.; Ryu, J.; Koo, M.; Choi, I.; Lee, S.H.; Byun, M.; Wang, Z.L. Highly-efficient, flexible piezoelectric PZT thin film nanogenerator on plastic substrates. *Adv. Mater.* **2014**, *26*, 2514–2520. [CrossRef]
14. Niu, X.; Jia, W.; Qian, S.; Zhu, J.; Zhang, J.; Hou, X.; Mu, J.; Geng, W.; Cho, J.; He, J. High-performance PZT-based stretchable piezoelectric nanogenerator. *ACS Sustain. Chem. Eng.* **2018**, *7*, 979–985. [CrossRef]
15. Kiat, J.-M.; Uesu, Y.; Dkhil, B.; Matsuda, M.; Malibert, C.; Calvarin, G. Monoclinic structure of unpoled morphotropic high piezoelectric PMN-PT and PZN-PT compounds. *Phys. Rev. B* **2002**, *65*, 064106. [CrossRef]
16. Xu, S.; Yeh, Y.-W.; Poirier, G.; McAlpine, M.C.; Register, R.A.; Yao, N. Flexible piezoelectric PMN–PT nanowire-based nanocomposite and device. *Nano Lett.* **2013**, *13*, 2393–2398. [CrossRef]
17. Hwang, G.T.; Park, H.; Lee, J.H.; Oh, S.; Park, K.I.; Byun, M.; Park, H.; Ahn, G.; Jeong, C.K.; No, K. Self-powered cardiac pacemaker enabled by flexible single crystalline PMN-PT piezoelectric energy harvester. *Adv. Mater.* **2014**, *26*, 4880–4887. [CrossRef]
18. Takenaka, T.; Maruyama, K.-I.; Sakata, K. ($Bi_{1/2}Na_{1/2}$) TiO_3-$BaTiO_3$ system for lead-free piezoelectric ceramics. *Jpn. J. Appl. Phys.* **1991**, *30*, 2236. [CrossRef]
19. Karaki, T.; Yan, K.; Miyamoto, T.; Adachi, M. Lead-free piezoelectric ceramics with large dielectric and piezoelectric constants manufactured from $BaTiO_3$ nano-powder. *Jpn. J. Appl. Phys.* **2007**, *46*, L97. [CrossRef]
20. Park, K.-I.; Xu, S.; Liu, Y.; Hwang, G.-T.; Kang, S.-J.L.; Wang, Z.L.; Lee, K.J. Piezoelectric $BaTiO_3$ thin film nanogenerator on plastic substrates. *Nano Lett.* **2010**, *10*, 4939–4943. [CrossRef]
21. Kim, J.; Lee, J.H.; Ryu, H.; Lee, J.H.; Khan, U.; Kim, H.; Kwak, S.S.; Kim, S.-W. High-Performance Piezoelectric, Pyroelectric, and Triboelectric Nanogenerators Based on P (VDF-TrFE) with Controlled Crystallinity and Dipole Alignment. *Adv. Funct. Mater.* **2017**, *27*, 1700702. [CrossRef]
22. Lee, J.H.; Ryu, H.; Kim, T.Y.; Kwak, S.S.; Yoon, H.J.; Kim, T.H.; Seung, W.; Kim, S.-W. Thermally Induced Strain-Coupled Highly Stretchable and Sensitive Pyroelectric Nanogenerators. *Adv. Energy Mater.* **2015**, *5*, 1500704. [CrossRef]
23. Lee, J.-H.; Lee, K.Y.; Kumar, B.; Tien, N.T.; Lee, N.-E.; Kim, S.-W. Highly sensitive stretchable transparent piezoelectric nanogenerators. *Energy Environ. Sci.* **2013**, *6*, 169–175. [CrossRef]
24. Datta, A.; Choi, Y.S.; Chalmers, E.; Ou, C.; Kar-Narayan, S. Piezoelectric Nylon-11 Nanowire Arrays Grown by Template Wetting for Vibrational Energy Harvesting Applications. *Adv. Funct. Mater.* **2017**, *27*, 1604262. [CrossRef]
25. Liao, W.-Q.; Tang, Y.-Y.; Li, P.-F.; You, Y.-M.; Xiong, R.-G. Competitive halogen bond in the molecular ferroelectric with large piezoelectric response. *J. Am. Chem. Soc.* **2018**, *140*, 3975–3980. [CrossRef]
26. Kim, D.; Han, S.A.; Kim, J.H.; Lee, J.H.; Kim, S.-W.; Lee, S.W. Biomolecular Piezoelectric Materials: From Amino Acids to Living Tissues. *Adv. Mater.* **2020**, *32*, 1906989. [CrossRef]
27. Lee, J.-H.; Lee, J.H.; Xiao, J.; Desai, M.S.; Zhang, X.; Lee, S.-W. Vertical self-assembly of polarized phage nanostructure for energy harvesting. *Nano Lett.* **2019**, *19*, 2661–2667. [CrossRef]
28. Lee, J.-H.; Heo, K.; Schulz-Schönhagen, K.; Lee, J.H.; Desai, M.S.; Jin, H.-E.; Lee, S.-W. Diphenylalanine peptide nanotube energy harvesters. *ACS Nano* **2018**, *12*, 8138–8144. [CrossRef]
29. Liu, Q.; Wang, X.-X.; Song, W.-Z.; Qiu, H.-J.; Zhang, J.; Fan, Z.; Yu, M.; Long, Y.-Z. Wireless Single-Electrode Self-Powered Piezoelectric Sensor for Monitoring. *ACS Appl. Mater. Interfaces* **2020**, *12*, 8288–8295. [CrossRef]

30. Jeong, C.K.; Hyeon, D.Y.; Hwang, G.-T.; Lee, G.-J.; Lee, M.-K.; Park, J.-J.; Park, K.-I. Nanowire-percolated piezoelectric copolymer-based highly transparent and flexible self-powered sensors. *J. Mater. Chem. A* **2019**, *7*, 25481–25489. [CrossRef]
31. Fuh, Y.-K.; Chen, P.-C.; Huang, Z.-M.; Ho, H.-C. Self-powered sensing elements based on direct-write, highly flexible piezoelectric polymeric nano/microfibers. *Nano Energy* **2015**, *11*, 671–677. [CrossRef]
32. Sachan, V.K.; Imam, S.A.; Beg, M. Energy-efficient communication methods in wireless sensor networks: A critical review. *Int. J. Comput. Appl.* **2012**, *39*, 35–48.
33. Mohammadi, B.; Yousefi, A.A.; Bellah, S.M. Effect of tensile strain rate and elongation on crystalline structure and piezoelectric properties of PVDF thin films. *Polym. Test.* **2007**, *26*, 42–50. [CrossRef]
34. Rathod, V.; Mahapatra, D.R.; Jain, A.; Gayathri, A. Characterization of a large-area PVDF thin film for electro-mechanical and ultrasonic sensing applications. *Sens. Actuators A Phys.* **2010**, *163*, 164–171. [CrossRef]
35. Nordin, N.I.; Ab Rahim, R.; Ralib, A.A.M. Flexible PVDF thin film as piezoelectric energy harvester. *Bull. Electr. Eng. Inform.* **2019**, *8*, 443–449. [CrossRef]
36. Wang, Y.; Fang, M.; Tian, B.; Xiang, P.; Zhong, N.; Lin, H.; Luo, C.; Peng, H.; Duan, C.G. Transparent PVDF-TrFE/Graphene Oxide Ultrathin Films with Enhanced Energy Harvesting Performance. *ChemistrySelect* **2017**, *2*, 7951–7955. [CrossRef]
37. Al-Saygh, A.; Ponnamma, D.; AlMaadeed, M.A.; Vijayan, P.; Karim, A.; Hassan, M.K. Flexible pressure sensor based on PVDF nanocomposites containing reduced graphene oxide-titania hybrid nanolayers. *Polymers* **2017**, *9*, 33. [CrossRef]
38. Xu, G.; Zhang, M.; Zhou, Q.; Chen, H.; Gao, T.; Li, C.; Shi, G. A small graphene oxide sheet/polyvinylidene fluoride bilayer actuator with large and rapid responses to multiple stimuli. *Nanoscale* **2017**, *9*, 17465–17470. [CrossRef]
39. Bystrov, V.S.; Bdikin, I.K.; Silibin, M.; Karpinsky, D.; Kopyl, S.; Paramonova, E.V.; Goncalves, G. Molecular modeling of the piezoelectric properties of ferroelectric composites containing polyvinylidene fluoride (PVDF) and either graphene or graphene oxide. *J. Mol. Model.* **2017**, *23*, 128. [CrossRef]
40. Zhu, Y.; Yang, B.; Liu, J.; Wang, X.; Chen, X.; Yang, C. An integrated flexible harvester coupled triboelectric and piezoelectric mechanisms using PDMS/MWCNT and PVDF. *J. Microelectromech. Syst.* **2015**, *24*, 513–515. [CrossRef]
41. Gusarova, E.; Viala, B.; Plihon, A.; Gusarov, B.; Gimeno, L.; Cugat, O. Flexible screen-printed piezoelectric P (VDF-TrFE) copolymer microgenerators for energy harvesting. In Proceedings of the 2015 Transducers-2015 18th International Conference on Solid-State Sensors, Actuators and Microsystems (TRANSDUCERS), Anchorage, AK, USA, 21–25 June 2015; pp. 1901–1904.
42. Zhong, H.; Xia, J.; Wang, F.; Chen, H.; Wu, H.; Lin, S. Graphene-piezoelectric material heterostructure for harvesting energy from water flow. *Adv. Funct. Mater.* **2017**, *27*, 1604226. [CrossRef]
43. Kim, S.; Towfeeq, I.; Dong, Y.; Gorman, S.; Rao, A.M.; Koley, G. P (VDF-TrFE) film on PDMS substrate for energy harvesting applications. *Appl. Sci.* **2018**, *8*, 213. [CrossRef]
44. Pi, Z.; Zhang, J.; Wen, C.; Zhang, Z.-B.; Wu, D. Flexible piezoelectric nanogenerator made of poly (vinylidenefluoride-co-trifluoroethylene)(PVDF-TrFE) thin film. *Nano Energy* **2014**, *7*, 33–41. [CrossRef]
45. Lee, J.H.; Lee, K.Y.; Gupta, M.K.; Kim, T.Y.; Lee, D.Y.; Oh, J.; Ryu, C.; Yoo, W.J.; Kang, C.Y.; Yoon, S.J. Highly stretchable piezoelectric-pyroelectric hybrid nanogenerator. *Adv. Mater.* **2014**, *26*, 765–769. [CrossRef]
46. Bhavanasi, V.; Kumar, V.; Parida, K.; Wang, J.; Lee, P.S. Enhanced piezoelectric energy harvesting performance of flexible PVDF-TrFE bilayer films with graphene oxide. *ACS Appl. Mater. Interfaces* **2016**, *8*, 521–529. [CrossRef] [PubMed]
47. Okoshi, T.; Chen, H.; Soldani, G.; Galletti, P.M.; Goddard, M. Microporous small diameter PVDF-TrFE vascular grafts fabricated by a spray phase inversion technique. *ASAIO J.* **1992**, *38*, M201–M206. [CrossRef]
48. Suwansumpan, D.; Manuspiya, H.; Laoratanakul, P.; Bhalla, A. *Induced Internal Bubble Shapes Affected Piezoelectric Behaviors of PVDF Films*; Advanced Materials Research, Trans Tech Publications Ltd.: Stafa-Zurich, Switzerland, 2008; pp. 101–104.
49. Cardoso, V.F.; Botelho, G.; Lanceros-Méndez, S. Nonsolvent induced phase separation preparation of poly (vinylidene fluoride-co-chlorotrifluoroethylene) membranes with tailored morphology, piezoelectric phase content and mechanical properties. *Mater. Des.* **2015**, *88*, 390–397. [CrossRef]

50. Chen, D.; Hang, M.; Chen, K.; Brown, K.; Zhang, J.X. Piezoelectric PVDF thin films with asymmetric microporous structures for pressure sensing. In Proceedings of the 2015 IEEE SENSORS, Busan, Korea, 1–4 November 2015; pp. 1–4.
51. Chen, D.; Zhang, J.X. Microporous polyvinylidene fluoride film with dense surface enables efficient piezoelectric conversion. *Appl. Phys. Lett.* **2015**, *106*, 193901. [CrossRef]
52. Correia, D.M.; Ribeiro, C.; Sencadas, V.; Vikingsson, L.; Gasch, M.O.; Ribelles, J.G.; Botelho, G.; Lanceros-Méndez, S. Strategies for the development of three dimensional scaffolds from piezoelectric poly (vinylidene fluoride). *Mater. Des.* **2016**, *92*, 674–681. [CrossRef]
53. Park, Y.J.; Kang, Y.S.; Park, C. Micropatterning of semicrystalline poly (vinylidene fluoride)(PVDF) solutions. *Eur. Polym. J.* **2005**, *41*, 1002–1012. [CrossRef]
54. Li, C.; Wu, P.-M.; Lee, S.; Gorton, A.; Schulz, M.J.; Ahn, C.H. Flexible dome and bump shape piezoelectric tactile sensors using PVDF-TrFE copolymer. *J. Microelectromech. Syst.* **2008**, *17*, 334–341.
55. Han, H.; Nakagawa, Y.; Takai, Y.; Kikuchi, K.; Tsuchitani, S. PVdf film micro fabrication for the robotics skin sensor having flexibility and high sensitivity. In Proceedings of the 2011 Fifth International Conference on Sensing Technology, Palmerston North, New Zealand, 28 November–1 December 2011; pp. 603–606.
56. Ong, W.; Ke, C.; Lim, P.; Kuarm, A.; Zeng, K.; Ho, G.W. Direct stamping and capillary flow patterning of solution processable piezoelectric polyvinylidene fluoride films. *Polymer* **2013**, *54*, 5330–5337. [CrossRef]
57. Sümer, B.; Koc, I.M. Fabrication of a flexible tactile sensor with micro-pillar array. *Procedia Eng.* **2015**, *120*, 134–137. [CrossRef]
58. Zabek, D.; Taylor, J.; Boulbar, E.L.; Bowen, C.R. Micropatterning of flexible and free standing polyvinylidene difluoride (PVDF) films for enhanced pyroelectric energy transformation. *Adv. Energy Mater.* **2015**, *5*, 1401891. [CrossRef]
59. Shuai, X.; Zhu, P.; Zeng, W.; Hu, Y.; Liang, X.; Zhang, Y.; Sun, R.; Wong, C.-P. Highly sensitive flexible pressure sensor based on silver nanowires-embedded polydimethylsiloxane electrode with microarray structure. *ACS Appl. Mater. Interfaces* **2017**, *9*, 26314–26324. [CrossRef]
60. Wu, Y.; Du, X.; Gao, R.; Li, J.; Li, W.; Yu, H.; Jiang, Z.; Wang, Z.; Tai, H. Self-polarization of PVDF film triggered by hydrophilic treatment for pyroelectric sensor with ultra-low piezoelectric noise. *Nanoscale Res. Lett.* **2019**, *14*, 72. [CrossRef]
61. Gallego, D.; Ferrell, N.J.; Hansford, D.J. Fabrication of piezoelectric polyvinylidene fluoride (PVDF) microstructures by soft lithography for tissue engineering and cell biology applications. *MRS Online Proc. Libr. Arch.* **2007**, 1002. [CrossRef]
62. Xu, J.; Dapino, M.J.; Gallego-Perez, D.; Hansford, D. Microphone based on polyvinylidene fluoride (PVDF) micro-pillars and patterned electrodes. *Sens. Actuators A Phys.* **2009**, *153*, 24–32. [CrossRef]
63. Canavese, G.; Stassi, S.; Cauda, V.; Verna, A.; Motto, P.; Chiodoni, A.; Marasso, S.L.; Demarchi, D. Different scale confinements of PVDF-TrFE as functional material of piezoelectric devices. *IEEE Sens. J.* **2013**, *13*, 2237–2244. [CrossRef]
64. Chen, X.; Shao, J.; Tian, H.; Li, X.; Tian, Y.; Wang, C. Flexible three-axial tactile sensors with microstructure-enhanced piezoelectric effect and specially-arranged piezoelectric arrays. *Smart Mater. Struct.* **2018**, *27*, 025018. [CrossRef]
65. Pariy, I.; Ivanova, A.; Shvartsman, V.; Lupascu, D.; Sukhorukov, G.; Surmeneva, M.; Surmenev, R. Poling and annealing of piezoelectric Poly (Vinylidene fluoride) micropillar arrays. *Mater. Chem. Phys.* **2020**, *239*, 122035. [CrossRef]
66. Fuh, Y.-K.; Chen, S.-Y.; Ye, J.-C. Massively parallel aligned microfibers-based harvester deposited via in situ, oriented poled near-field electrospinning. *Appl. Phys. Lett.* **2013**, *103*, 033114. [CrossRef]
67. Fuh, Y.-K.; Ye, J.-C.; Chen, P.-C.; Huang, Z.-M. A highly flexible and substrate-independent self-powered deformation sensor based on massively aligned piezoelectric nano-/microfibers. *J. Mater. Chem. A* **2014**, *2*, 16101–16106. [CrossRef]
68. Huang, Y.; Ding, Y.; Bian, J.; Su, Y.; Zhou, J.; Duan, Y.; Yin, Z. Hyper-stretchable self-powered sensors based on electrohydrodynamically printed, self-similar piezoelectric nano/microfibers. *Nano Energy* **2017**, *40*, 432–439. [CrossRef]
69. Fabriani, F.; Chinnam, K.C.; Casalotti, A.; Lanzara, G. *Effect of Electrospun PVDF-Fibers Orientation for Vibration Sensing*; IOP Conference Series: Materials Science and Engineering; IOP Publishing: Bristol, UK, 2019; p. 012056.

70. Yuan, Y.; Dai, Y.; Xu, M.; Wang, Z.; Chen, Z. Highly Stretchable Piezoelectric Strain Sensor with Dual Wavy Structures of PVDF Microfibers. In Proceedings of the 2020 IEEE 4th Information Technology, Networking, Electronic and Automation Control Conference (ITNEC), Chongqing, China, 12–14 June 2020; pp. 2418–2422.
71. Chen, D.; Sharma, T.; Zhang, J.X. Mesoporous surface control of PVDF thin films for enhanced piezoelectric energy generation. *Sens. Actuators A Phys.* **2014**, *216*, 196–201. [CrossRef]
72. Lee, J.-H.; Yoon, H.J.; Kim, T.Y.; Gupta, M.K.; Lee, J.H.; Seung, W.; Ryu, H.; Kim, S.-W. Micropatterned P (VDF-TrFE) film-based piezoelectric nanogenerators for highly sensitive self-powered pressure sensors. *Adv. Funct. Mater.* **2015**, *25*, 3203–3209. [CrossRef]
73. Choi, Y.-Y.; Yun, T.G.; Qaiser, N.; Paik, H.; Roh, H.S.; Hong, J.; Hong, S.; Han, S.M.; No, K. Vertically aligned P (VDF-TrFE) core-shell structures on flexible pillar arrays. *Sci. Rep.* **2015**, *5*, 10728. [CrossRef]
74. Chen, X.; Tian, H.; Li, X.; Shao, J.; Ding, Y.; An, N.; Zhou, Y. A high performance P (VDF-TrFE) nanogenerator with self-connected and vertically integrated fibers by patterned EHD pulling. *Nanoscale* **2015**, *7*, 11536–11544. [CrossRef]
75. Cha, S.; Kim, S.M.; Kim, H.; Ku, J.; Sohn, J.I.; Park, Y.J.; Song, B.G.; Jung, M.H.; Lee, E.K.; Choi, B.L. Porous PVDF as effective sonic wave driven nanogenerators. *Nano Lett.* **2011**, *11*, 5142–5147. [CrossRef]
76. Cauda, V.; Stassi, S.; Bejtka, K.; Canavese, G. Nanoconfinement: An effective way to enhance PVDF piezoelectric properties. *ACS Appl. Mater. Interfaces* **2013**, *5*, 6430–6437. [CrossRef]
77. Fu, C.; Wang, X.; Shi, X.; Ran, X. The induction of poly (vinylidene fluoride) electroactive phase by modified anodic aluminum oxide template nanopore surface. *RSC Adv.* **2015**, *5*, 87429–87436. [CrossRef]
78. Zhao, P.; Wang, S.; Kadlec, A. Piezoelectric and dielectric properties of nanoporous polyvinylidence fluoride (PVDF) films. In *Behavior and Mechanics of Multifunctional Materials and Composites 2016, Proceedings of the SPIE Smart Structures and Materials + Nondestructive Evaluation and Health Monitoring, Las Vegas, NV, USA, 21–23 March 2016*; International Society for Optics and Photonics: Washington, DC, USA, 2016; p. 98000P.
79. Li, H.; Zhang, Y.; Dai, H.; Tong, W.; Zhou, Y.; Zhao, J.; An, Q. A self-powered porous ZnS/PVDF-HFP mechanoluminescent composite film that converts human movement into eye-readable light. *Nanoscale* **2018**, *10*, 5489–5495. [CrossRef]
80. Chang, C.; Tran, V.H.; Wang, J.; Fuh, Y.-K.; Lin, L. Direct-write piezoelectric polymeric nanogenerator with high energy conversion efficiency. *Nano Lett.* **2010**, *10*, 726–731. [CrossRef]
81. Wang, Y.; Zheng, J.; Ren, G.; Zhang, P.; Xu, C. A flexible piezoelectric force sensor based on PVDF fabrics. *Smart Mater. Struct.* **2011**, *20*, 045009. [CrossRef]
82. Hadimani, R.L.; Bayramol, D.V.; Sion, N.; Shah, T.; Qian, L.; Shi, S.; Siores, E. Continuous production of piezoelectric PVDF fibre for e-textile applications. *Smart Mater. Struct.* **2013**, *22*, 075017. [CrossRef]
83. Fuh, Y.-K.; Ye, J.-C.; Chen, P.-C.; Ho, H.-C.; Huang, Z.-M. Hybrid energy harvester consisting of piezoelectric fibers with largely enhanced 20 V for wearable and muscle-driven applications. *ACS Appl. Mater. Interfaces* **2015**, *7*, 16923–16931. [CrossRef] [PubMed]
84. Mokhtari, F.; Latifi, M.; Shamshirsaz, M. Electrospinning/electrospray of polyvinylidene fluoride (PVDF): Piezoelectric nanofibers. *J. Text. Inst.* **2016**, *107*, 1037–1055. [CrossRef]
85. Bera, B.; Sarkar, M.D. PVDF based Piezoelectric Nanogenerator as a new kind of device for generating power from renewable resources. *IOSR J. Polym. Text. Eng. (IOSR-JPTE)* **2017**, *4*, 1–5. [CrossRef]
86. Serairi, L.; Gu, L.; Qin, Y.; Lu, Y.; Basset, P.; Leprince-Wang, Y. Flexible piezoelectric nanogenerators based on PVDF-TrFE nanofibers. *Eur. Phys. J. Appl. Phys.* **2017**, *80*, 30901. [CrossRef]
87. Yaman, M.; Khudiyev, T.; Ozgur, E.; Kanik, M.; Aktas, O.; Ozgur, E.O.; Deniz, H.; Korkut, E.; Bayindir, M. Arrays of indefinitely long uniform nanowires and nanotubes. *Nat. Mater.* **2011**, *10*, 494–501. [CrossRef]
88. Liew, W.H.; Mirshekarloo, M.S.; Chen, S.; Yao, K.; Tay, F.E.H. Nanoconfinement induced crystal orientation and large piezoelectric coefficient in vertically aligned P (VDF-TrFE) nanotube array. *Sci. Rep.* **2015**, *5*, 09790. [CrossRef] [PubMed]
89. Pan, C.-T.; Yen, C.-K.; Wang, S.-Y.; Lai, Y.-C.; Lin, L.; Huang, J.; Kuo, S.-W. Near-field electrospinning enhances the energy harvesting of hollow PVDF piezoelectric fibers. *RSC Adv.* **2015**, *5*, 85073–85081. [CrossRef]
90. Wu, C.-M.; Chou, M.-H.; Zeng, W.-Y. Piezoelectric response of aligned electrospun polyvinylidene fluoride/carbon nanotube nanofibrous membranes. *Nanomaterials* **2018**, *8*, 420. [CrossRef] [PubMed]
91. Mao, Y.; Zhao, P.; McConohy, G.; Yang, H.; Tong, Y.; Wang, X. Sponge-like piezoelectric polymer films for scalable and integratable nanogenerators and self-powered electronic systems. *Adv. Energy Mater.* **2014**, *4*, 1301624. [CrossRef]

92. Bhavanasi, V.; Kusuma, D.Y.; Lee, P.S. Polarization Orientation, Piezoelectricity, and Energy Harvesting Performance of Ferroelectric PVDF-TrFE Nanotubes Synthesized by Nanoconfinement. *Adv. Energy Mater.* **2014**, *4*, 1400723. [CrossRef]
93. Rahman, M.A.; Chung, G.-S. Synthesis of PVDF-graphene nanocomposites and their properties. *J. Alloys Compd.* **2013**, *581*, 724–730. [CrossRef]
94. Al-Hazmi, F.S.; de Leeuw, D.M.; Al-Ghamdi, A.; Shokr, F. Synthesis and characterization of novel Cu2O/PVDF nanocomposites for flexible ferroelectric organic electronic memory devices. *Curr. Appl. Phys.* **2017**, *17*, 1181–1188. [CrossRef]
95. Chinya, I.; Pal, A.; Sen, S. Polyglycolated zinc ferrite incorporated poly (vinylidene fluoride)(PVDF) composites with enhanced piezoelectric response. *J. Alloys Compd.* **2017**, *722*, 829–838. [CrossRef]
96. El Achaby, M.; Arrakhiz, F.; Vaudreuil, S.; Essassi, E.; Qaiss, A. Piezoelectric β-polymorph formation and properties enhancement in graphene oxide–PVDF nanocomposite films. *Appl. Surf. Sci.* **2012**, *258*, 7668–7677. [CrossRef]
97. Silibin, M.; Bystrov, V.; Karpinsky, D.; Nasani, N.; Goncalves, G.; Gavrilin, I.; Solnyshkin, A.; Marques, P.; Singh, B.; Bdikin, I. Local mechanical and electromechanical properties of the P (VDF-TrFE)-graphene oxide thin films. *Appl. Surf. Sci.* **2017**, *421*, 42–51. [CrossRef]
98. Lee, M.; Chen, C.Y.; Wang, S.; Cha, S.N.; Park, Y.J.; Kim, J.M.; Chou, L.J.; Wang, Z.L. A hybrid piezoelectric structure for wearable nanogenerators. *Adv. Mater.* **2012**, *24*, 1759–1764. [CrossRef] [PubMed]
99. Fu, J.; Hou, Y.; Gao, X.; Zheng, M.; Zhu, M. Highly durable piezoelectric energy harvester based on a PVDF flexible nanocomposite filled with oriented $BaTi_2O_5$ nanorods with high power density. *Nano Energy* **2018**, *52*, 391–401. [CrossRef]
100. Ding, R.; Zhang, X.; Chen, G.; Wang, H.; Kishor, R.; Xiao, J.; Gao, F.; Zeng, K.; Chen, X.; Sun, X.W. High-performance piezoelectric nanogenerators composed of formamidinium lead halide perovskite nanoparticles and poly (vinylidene fluoride). *Nano Energy* **2017**, *37*, 126–135. [CrossRef]
101. Kim, H.; Fernando, T.; Li, M.; Lin, Y.; Tseng, T.-L.B. Fabrication and characterization of 3D printed $BaTiO_3$/PVDF nanocomposites. *J. Compos. Mater.* **2018**, *52*, 197–206. [CrossRef]
102. Xue, J.; Wu, L.; Hu, N.; Qiu, J.; Chang, C.; Atobe, S.; Fukunaga, H.; Watanabe, T.; Liu, Y.; Ning, H. Evaluation of piezoelectric property of reduced graphene oxide (rGO)–poly (vinylidene fluoride) nanocomposites. *Nanoscale* **2012**, *4*, 7250–7255.
103. Harstad, S.; D'Souza, N.; Soin, N.; El-Gendy, A.A.; Gupta, S.; Pecharsky, V.K.; Shah, T.; Siores, E.; Hadimani, R.L. Enhancement of β-phase in PVDF films embedded with ferromagnetic Gd5Si4 nanoparticles for piezoelectric energy harvesting. *AIP Adv.* **2017**, *7*, 056411. [CrossRef]
104. Singh, H.H.; Singh, S.; Khare, N. Enhanced β-phase in PVDF polymer nanocomposite and its application for nanogenerator. *Polym. Adv. Technol.* **2018**, *29*, 143–150. [CrossRef]
105. Xiao, Z.; Guo, H.; He, H.; Liu, Y.; Li, X.; Zhang, Y.; Yin, H.; Volkov, A.V.; He, T. Unprecedented scaling/fouling resistance of omniphobic polyvinylidene fluoride membrane with silica nanoparticle coated micropillars in direct contact membrane distillation. *J. Membr. Sci.* **2020**, 117819. [CrossRef]
106. Lee, D.-Y.; Kim, H.; Li, H.-M.; Jang, A.-R.; Lim, Y.-D.; Cha, S.N.; Park, Y.J.; Kang, D.J.; Yoo, W.J. Hybrid energy harvester based on nanopillar solar cells and PVDF nanogenerator. *Nanotechnology* **2013**, *24*, 175402. [CrossRef]
107. Melilli, G.; Gorse, D.; Galifanova, A.; Oral, O.; Balanzat, E.; Doare, D.; Tabellout, M.; Bechelany, M.; Lairez, D.; Je, W. Enhanced Piezoelectric Response in Nanostructured Ni/PVDF Films. *J. Mater. Sci. Eng.* **2018**, *7*. [CrossRef]
108. Koç, İ.M.; Akça, E. Design of a piezoelectric based tactile sensor with bio-inspired micro/nano-pillars. *Tribol. Int.* **2013**, *59*, 321–331.
109. Salehi-Khojin, A.; Jalili, N. A comprehensive model for load transfer in nanotube reinforced piezoelectric polymeric composites subjected to electro-thermo-mechanical loadings. *Compos. Part B Eng.* **2008**, *39*, 986–998. [CrossRef]
110. Shi, K.; Sun, B.; Huang, X.; Jiang, P. Synergistic effect of graphene nanosheet and $BaTiO_3$ nanoparticles on performance enhancement of electrospun PVDF nanofiber mat for flexible piezoelectric nanogenerators. *Nano Energy* **2018**, *52*, 153–162. [CrossRef]
111. Khudiyev, T.; Ozgur, E.; Yaman, M.; Bayindir, M. Structural coloring in large scale core–shell nanowires. *Nano Lett.* **2011**, *11*, 4661–4665. [CrossRef] [PubMed]

112. Abbasipour, M.; Khajavi, R.; Yousefi, A.A.; Yazdanshenas, M.E.; Razaghian, F. The piezoelectric response of electrospun PVDF nanofibers with graphene oxide, graphene, and halloysite nanofillers: A comparative study. *J. Mater. Sci. Mater. Electron.* **2017**, *28*, 15942–15952. [CrossRef]
113. Cheon, S.; Kang, H.; Kim, H.; Son, Y.; Lee, J.Y.; Shin, H.J.; Kim, S.W.; Cho, J.H. High-Performance Triboelectric Nanogenerators Based on Electrospun Polyvinylidene Fluoride–Silver Nanowire Composite Nanofibers. *Adv. Funct. Mater.* **2018**, *28*, 1703778. [CrossRef]
114. Bera, B.; Sarkar, M.D. Gold nanoparticle doped PVDF nanofiber preparation of concurrently harvesting light and mechanical energy. *IOSR J. Appl. Phys. (IOSR-JAP)* **2017**, *9*, 5–12. [CrossRef]
115. Ji, S.H.; Cho, J.H.; Jeong, Y.H.; Paik, J.-H.; Do Yun, J.; Yun, J.S. Flexible lead-free piezoelectric nanofiber composites based on BNT-ST and PVDF for frequency sensor applications. *Sens. Actuators A Phys.* **2016**, *247*, 316–322. [CrossRef]
116. Bafqi, M.S.S.; Bagherzadeh, R.; Latifi, M. Fabrication of composite PVDF-ZnO nanofiber mats by electrospinning for energy scavenging application with enhanced efficiency. *J. Polym. Res.* **2015**, *22*, 130. [CrossRef]
117. Garain, S.; Jana, S.; Sinha, T.K.; Mandal, D. Design of in situ poled Ce^{3+}-doped electrospun PVDF/graphene composite nanofibers for fabrication of nanopressure sensor and ultrasensitive acoustic nanogenerator. *ACS Appl. Mater. Interfaces* **2016**, *8*, 4532–4540. [CrossRef]
118. Alluri, N.R.; Saravanakumar, B.; Kim, S.-J. Flexible, Hybrid Piezoelectric Film ($BaTi_{(1-x)}Zr_xO_3$)/PVDF Nanogenerator as a Self-Powered Fluid Velocity Sensor. *ACS Appl. Mater. Interfaces* **2015**, *7*, 9831–9840. [CrossRef] [PubMed]
119. Ye, S.; Cheng, C.; Chen, X.; Chen, X.; Shao, J.; Zhang, J.; Hu, H.; Tian, H.; Li, X.; Ma, L. High-performance piezoelectric nanogenerator based on microstructured P (VDF-TrFE)/BNNTs composite for energy harvesting and radiation protection in space. *Nano Energy* **2019**, *60*, 701–714. [CrossRef]
120. Kang, H.B.; Han, C.S.; Pyun, J.C.; Ryu, W.H.; Kang, C.-Y.; Cho, Y.S. (Na, K) NbO_3 nanoparticle-embedded piezoelectric nanofiber composites for flexible nanogenerators. *Compos. Sci. Technol.* **2015**, *111*, 1–8. [CrossRef]